Asian Journal of Chemistry; Vol. 33, No. 9 (2021), 2073-2081

ASIAN JOURNAL OF CHEMISTRY

https://doi.org/10.14233/ajchem.2021.23284

Density Functional Theory (DFT) Study of Electronic and Optical Properties of Donor (D)-Acceptor (A) Monomers Based on 2,7-Carbazole Linked with Some Acceptor Groups

CHARITHA ANNAM[1], N. MURALI KRISHNA[2] and MANNAM SUBBARAO[1,*]

[1]Department of Chemistry, Acharya Nagarjuna University, Nagarjuna Nagar-522510, India
[2]Department of Chemistry, V.R. Siddhartha Engineering College, Kanuru, Vijayawada-520007, India

*Corresponding author: E-mail: mannamsrao@gmail.com

Received: 30 April 2021; *Accepted*: 18 June 2021; *Published online*: 20 August 2021; AJC-20468

In present study, a progression of low bandgap carbazole molecules was developed and rendered to increase their performance for organic solar cells. Thus, a design of D-A monomers from 2,7-carbazole donors (D) and a few acceptors (A) based D-A monomers was attempted. The calculation of the electronic and optical properties of the D-A monomers considered was based on the techniques of DFT and TD-DFT at the level of B3LYP with a basis set of 6-31G (d) in the gas and chlorobenzene. The HOMO and LUMO orbital energies, the bandgap energy (E_g), and the open-circuit voltage (V_{OC}) were calculated in the gas and solvent phase. The impacts of the acceptor groups on the calculations and optoelectronic properties of these D-A monomers are discussed in the study of the link between the electronic structure and the optoelectronic properties. Some of these D-A monomers suggested that the after-effects of this work are a good possibility for formation of organic solar cells.

Keywords: Carbazole, D-A monomers, Electronic properties, DFT, TD-DFT, HOMO and LUMO.

INTRODUCTION

Due to their ability to achieve high electrical conductivity by doping, π-conjugated linear polymers, such as polyacetylene, poly(*p*-phenylene), poly(*p*-phenylene vinylene), poly(phenylene sulfide), polypyrrole, polyaniline and polythiophene have drawn a lot of attention [1-5]. Since late, there has been a great deal of interest in the advancement of organic materials for use in the electronic industries. Poly(vinyl carbazole) has been used in several semiconductor applications. Studies have shown that this material could be used in electroluminescent devices as a hollow transport material [6], a light emitting material [7] or a wide bandgap energy transfer donor [8-11]. Until late, carbazole main chain polymers have received little consideration, despite the potential advantages that such polymers could have in the examination poly(vinyl carbazole). Carbazole based monomers are more significant in applications involving organic solar cells (OSCs) because carbazole derivatives have higher transporting properties, electron-rich (*p*-type) material, higher photo-conductivity, thermal stability and chemical constancy [12-26].

For example, 3,6-position carbazole reacts rapidly with different electrophiles and as needed, various forms of linear and branched poly(3,6-carbazole) derivatives have been shown to exhibit strong redox activities and non-linear optical or photorefractive properties [17,18]. These highlights also were applied to organic light-emitting diodes (OLEDs) [19]. Intriguingly more, during the head on investigations of 2,7-dihalogen carbazole monomers, the poly(2,7-carbazole) subsidiaries were found [20,21]. A progression of 2,7-carbazole based copolymers was incorporated and a portion of them exhibited better semiconducting properties in organic field-impact semiconductors (OFETs), bulk heterojunction (BHJ) sun-oriented cells, and thermoelectric devices when compared with the counter 3,6-carbazole-based polymers [22-25]. However, this primary relation between 3,6-carbazole and 2,7-carbazole has not yet been clarified in the perovskite solar cells (PSCs) in the light of the emerging new devices.

In the present research, some attempts have been made to build new donor-acceptor (D-A) oligomer structures through the use of 9*H*-carbazole as a donor and benzo[*c*][1,2,5] oxadiazole (BCO); benzo[*c*][1,2,5]thiadiazole (BCT); benzo[*c*][1,2,5]-

selenadiazole (BCS); [1,2,5]oxadiazolo[3,4-*c*]pyridine (OCP); [1,2,5]thiadiazolo[3,4-*c*]pyridine (TCP); [1,2,5]selenadiazolo-[3,4-*c*]pyridine (SCP); [1,2,5] oxadiazolo[3,4-*d*]pyridazine (ODP); [1,2,5] thiadiazolo[3,4-*d*]pyridazine (TDP) as electron acceptors of 3,6-linkage carbazole oligomers.

The HOMO and LUMO level energies were examined and the hole energy is assessed as the contrast between the HOMO and LUMO energies ($E_{gap} = |E_{HOMO} - E_{LUMO}|$). The open-circuit voltage (V_{oc}) is calculated with the contrast between the HOMO of D-A monomers and the LUMO of PCBM (phenyl-C61-butyric acid methyl ester). PCBM is commonly used in solar cell devices as an acceptor; this acceptor has the part of tolerating the donor's electrons and ensures charge partition accordingly and because of its dissolvability in most natural solvents. All computations were completed utilizing the Gaussian 09W computational quantum chemistry software program.

COMPUTATIONAL METHODS

The calculations and the optoelectronic properties of all atoms were determined by the Gaussian09W program upheld by Gauss View 5.0 [26] utilizing a hybrid density functional [27] and Becke's three-parameter exchange functional joined with the LYP relationship useful (B3LYP) and with a 6-31G(d) basis set in the gas and solvent phase. The HOMO, LUMO and bandgap energies were additionally reasoned from the optimized structures. Furthermore, the impacts of solvents on the underlying properties were concentrated by methods for the self-consistent reaction-field (SCRF) technique dependent on PCM created by Tomasi *et al.* [28,29]. These useful and basis set mixes were picked because of previous work on the D-A framework, demonstrating that they performed enough to portray the deal properties, for example, the general security over a scope of dissolvable polarities and optical properties including the absorption spectra.

The vertical electronic excitation spectra, including wavelengths, oscillator qualities, and fundamental arrangement task, were methodically studied utilizing TD-DFT calculation with the 6-31G (d) basis set on the completely DFT-enhanced structure of the ground state [30-32]. Indeed, these figuring strategies have been effectively applied to other formed natural particles and polymers [33].

RESULTS AND DISCUSSION

Geometric properties: The geometry optimized structures of D-A monomers obtained by DFT/B3LYP method with 6-31G(d) basis set in both gas and solvent phase are depicted in Figs. 1 and 2. The selected dihedral angle (θ_i) and bond distance (d_{BL}) parameters that exist between the donor and acceptor moieties are presented in Table-1. The results indicate that all the studied monomers maintained non-planar expect CB-ODP, CB-TDP and CB-SDP in both gas and solvent (≈180º). It was somewhat surprising that our geometry optimization led to a non-planar structure for 2,7-linkage polycarbazoles in opposition to an earlier observation. The torsion angle between the connected carbazole units is found to be insensitive to the way of linkage and the degree of polymerization and ranges from 146º to ≈180º in gas and the solvent. The monomers 2,7-CB-ODP, CB-TDP and CB-SDP torsion angles have ≈180º

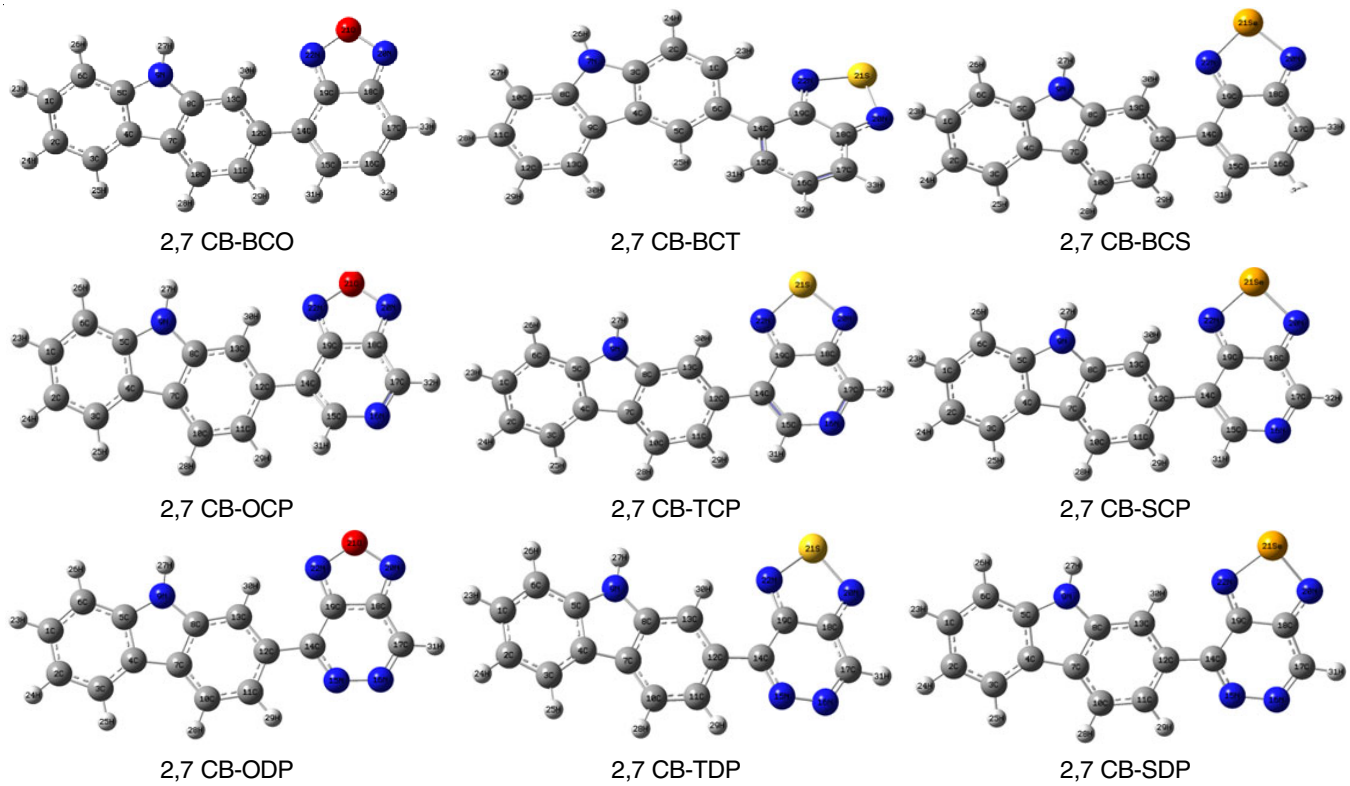

Fig. 1. Optimized molecular structures obtained by DFT/B3LYP/6-31G of the 2,7 linkage carbazole copolymer monomers (D-A) in gas phase

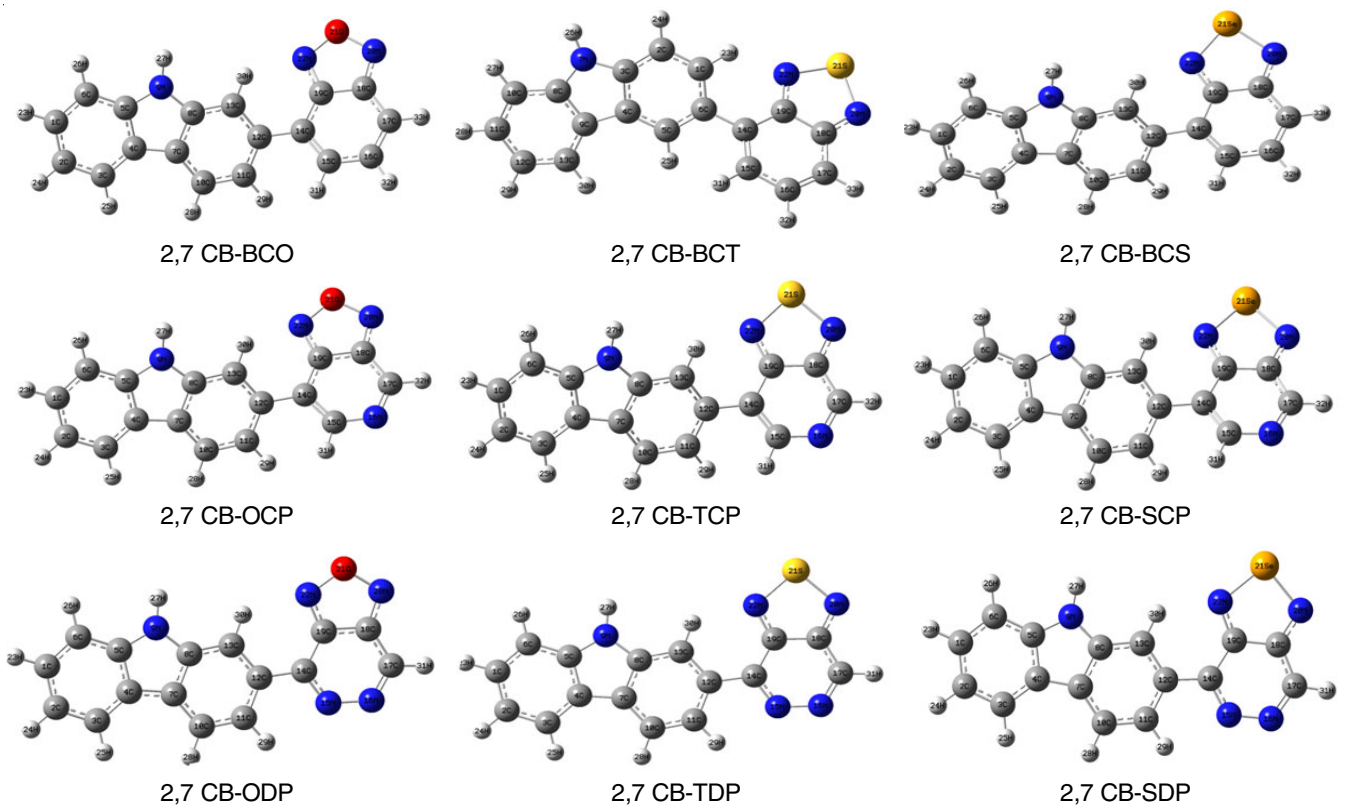

Fig. 2. Optimized geometry structures obtained by DFT/B3LYP/6-31G of the 2,7 linkage carbazole copolymer monomers (D-A) in chlorobenzene

TABLE-1
DIHEDRAL ANGLE (θ), BRIDGE LENGTH (d_B) AND DIPOLE MOMENTS (μ) FOR MODEL POLYMER MONOMERS CALCULATED BY DFT/B3LYP/6-31G LEVEL FOR 2, 7-CARBAZOLE BASED POLYMER MONOMERS

Polymer	θ (°)		d_B		μ debye	
	Gas	Chloro benzene	Gas	Chloro benzene	Gas	Sol
2,7-CB-BCO	154.48	150.69	1.47973	1.48016	–	4.5856
2,7-CB-BCT	146.04	143.58	1.48204	1.48226	3.2862	4.0307
2,7-CB-BCS	150.54	147.45	1.48341	1.48394	1.0087	1.2881
2,7-CB-OCP	156.54	152.97	1.47556	1.47540	3.3078	3.4596
2,7-CB-TCP	150.90	147.84	1.47896	1.47907	2.8922	3.3846
2,7-CB-SCP	153.54	149.81	1.47984	1.47992	3.3229	4.1655
2,7-CB-ODP	179.99	179.99	1.46650	1.46591	3.6946	4.4747
2,7-CB-TDP	179.99	179.99	1.47252	1.47301	4.5278	5.8879
2,7-CB-SDP	179.99	179.99	1.47348	1.47462	5.3082	7.0992

shows, an out-of-plane orientation relative to the plane of conjugation and the electron-donating effect of the oxygen (O), sulfur (S) and selenium (Se).

Optoelectronic properties

Frontier molecular orbital's: It's critical to look at the frontier molecular orbital (FMO) density since this can give us data about excitation properties by showing how the charge move happened by the side of the particle chain. The orbital density plots of the HOMO and LUMO of the examined monomers appear in Figs. 3 and 4 in the gas and solvent phase. It is noted that the FMO of all monomers has undifferentiated from circulation attributes, for example, the HOMOs have a π-holding character inside the D-A monomer and a π-antibonding character between the donor and acceptor. Though, the LUMO for the most part has a π-antibonding character inside the acceptor and a π-bonding character between the donors. The HOMO and LUMO electron densities are conveyed completely over the monomers.

Electronic properties: To consider the electronic properties of the organic molecules utilized in photovoltaic cells as organic solar cells, the HOMO and LUMO bandgap energies are helpful boundaries for this investigation. The HOMO and LUMO energies were gotten by DFT/B3LYP method with 6-31G(d) basis sets and their information is summed up with the bandgap energies of all D-A monomers in Table-2. We note that the HOMO and LUMO values going from - 5.5398 to – 5.9336 eV and from - 2.6641 to - 3.6578 eV in gas and - 5.5298 eV to - 5.8587 and from - 2.7253 to - 3.6851 eV, respectively. The LUMO energy values of all D-A monomers were

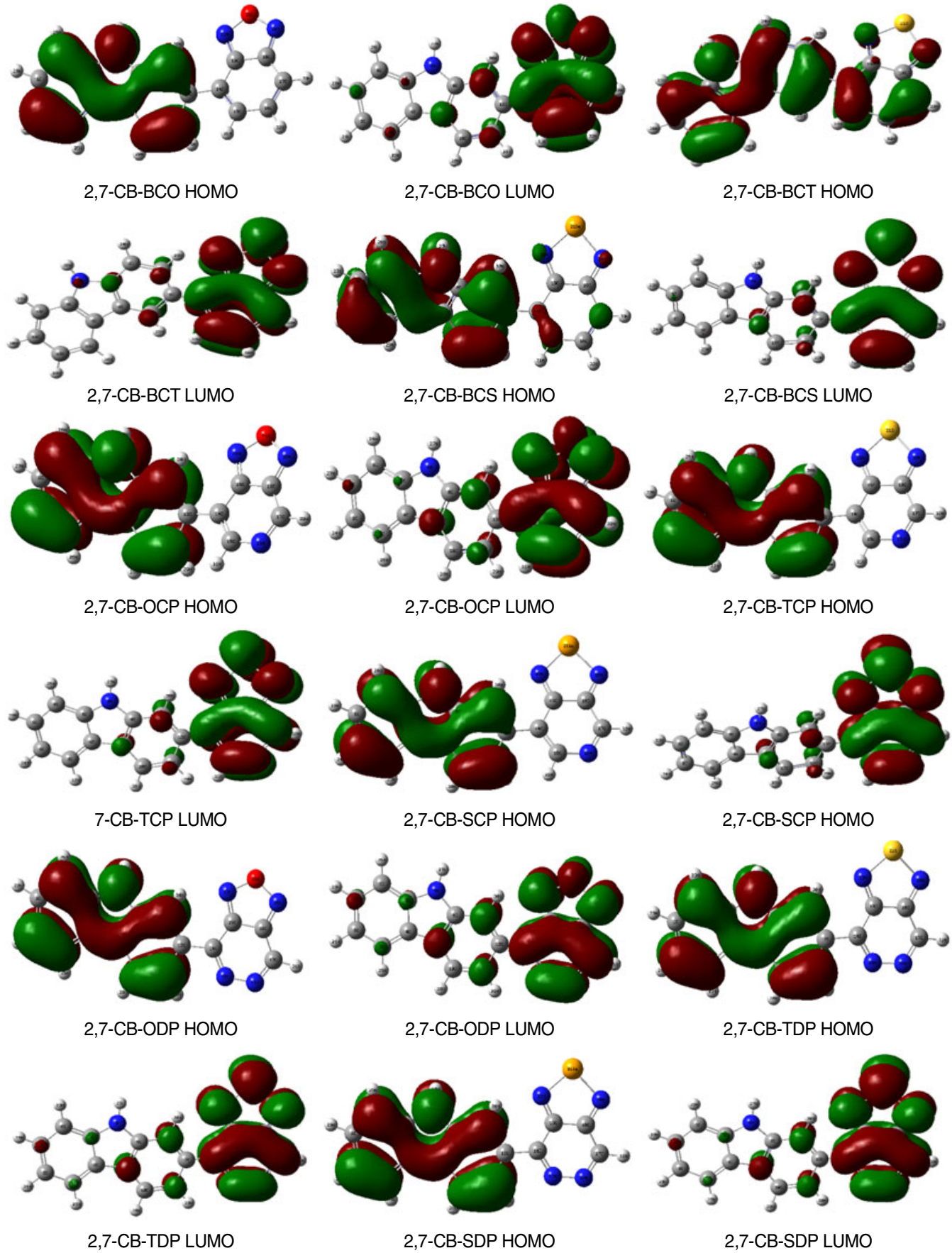

Fig. 3. The HOMO and LUMO orbitals contour plots calculated by DFT/B3LYP method with 6-31G (d) basis set for the 2,7 linkage carbazole monomers (D-A) in gas phase

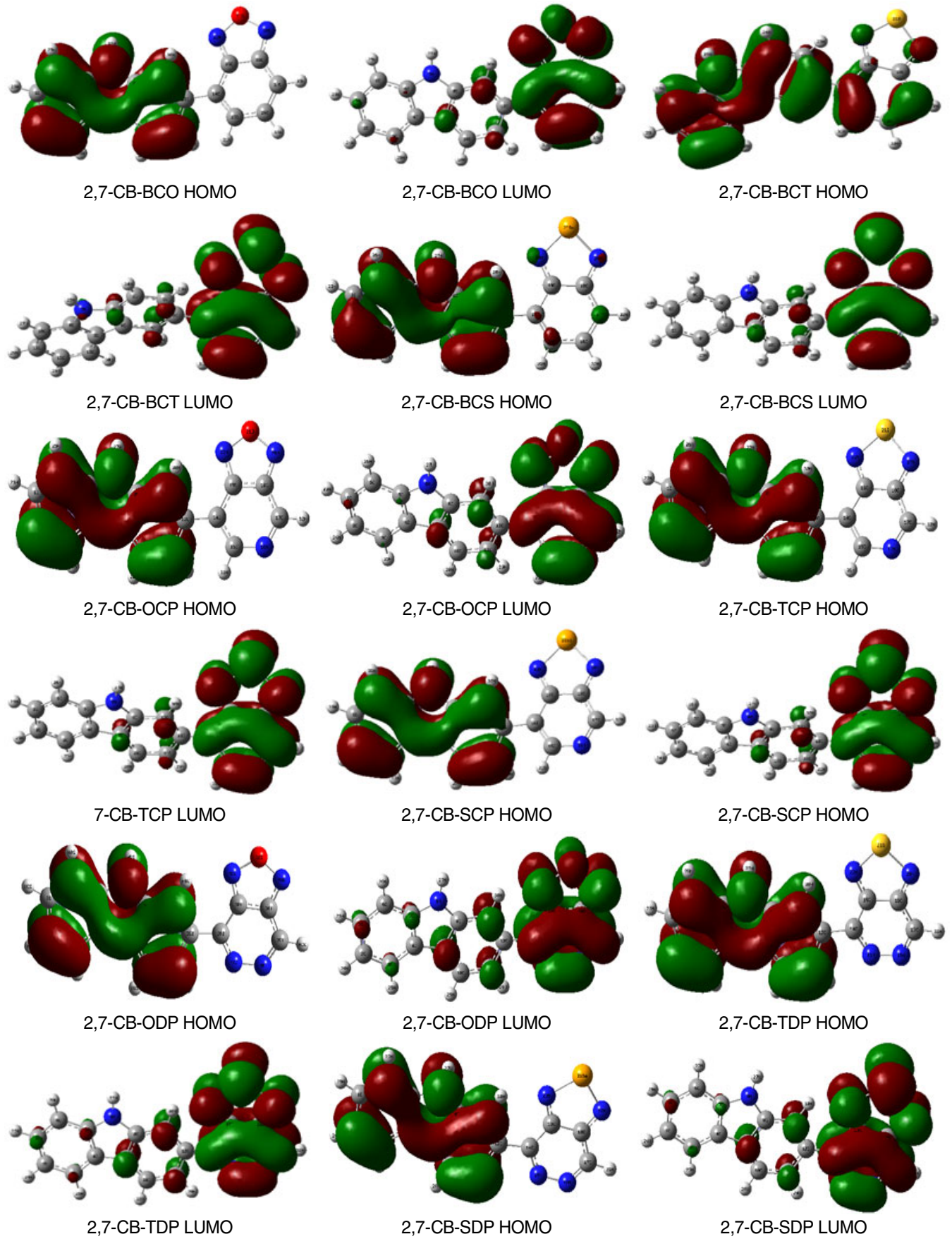

Fig. 4. The HOMO and LUMO orbitals contour plots calculated by DFT/B3LYP method with 6-31G (d) basis set for the 2,7 linkage carbazole monomers (D-A) in chlorobenzene

TABLE-2
HOMO AND LUMO ENERGY LEVELS (eV) AND BAND GAP ENERGIES (E_g) (eV) FOR D-A MONOMERS CALCULATED BY DFT/B3LYP METHOD WITH 6-31G BASIS SET

D-A polymer monomers	Gas			Chlorobenzene		
	HOMO	LUMO	E_g	HOMO	LUMO	E_g
2,7-CB-BCO	-5.7240	-2.7783	2.9457	-5.7129	-2.8739	2.8390
2,7-CB-BCT	-5.7240	-2.7784	2.9456	-5.5298	-2.7767	2.7531
2,7-CB-BCS	-5.5398	-2.6641	2.8757	-5.6144	-2.7253	2.8891
2,7-CB-OCP	-5.8636	-3.2703	2.5933	-5.6620	-3.6674	1.9946
2,7-CB-TCP	-5.7281	-3.2246	2.5035	-5.7134	-3.2562	2.4572
2,7-CB-SCP	-5.6647	-3.1237	2.5410	-5.6808	-3.1378	2.5430
2,7-CB-ODP	-5.9336	-3.6578	2.2758	-5.8587	-3.6851	2.1736
2,7-CB-TDP	-5.7763	-3.6070	2.1693	-5.7684	-3.5898	2.1786
2,7-CB-SDP	-5.7053	-3.4997	2.2056	-5.7276	-3.4674	2.2602

higher than the PCBMM acceptor values overall. Fig. 5 shows the energy orbital's for the considered monomers and the conducting band levels (LUMO) of PCBM.

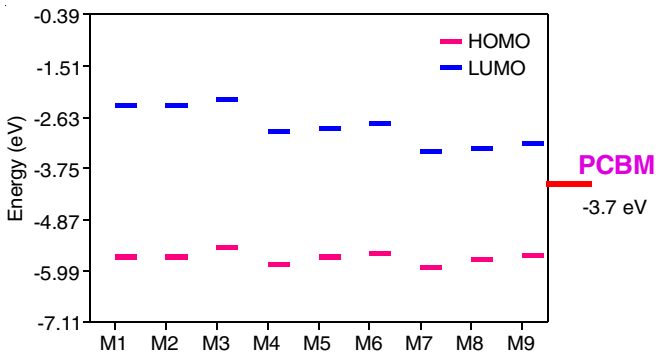

Fig. 5. The energies of the frontier orbital's HOMO and LUMO for the D-A monomers and conduction band levels of PCBM in gas phase. (M1 = 2,7-CB-BCO; M2 = 2,7-CB-BCT; M3 = 2,7-CB-BCS; M4 = 2,7-CB-OCP; M5 = 2,7-CB-TCP; M6 = 2,7-CB-SCP; M7 = 2,7-CB-ODP; M8 = 2,7-CB-TDP; M9 = 2,7-CB-SDP)

The determined bandgap energies (E_g) of the contemplated intensify go from 2.1693 to 2.9457 eV and 1.9946 to 2.8891 eV in the gas and solvent phase, respectively. The determined bandgap energy (E_g) of the monomers the following order: 2,7-CB-BCO > 2,7-CB-BCT > 2,7-CB-BCS > 2,7-CB-OCP > 2,7-CB-SCP > 2,7-CB-TCP > 2,7-CB-ODP > 2,7-CB-SDP > 2,7-CB-TDP in gas. Also, the smallest bandgap energy has been noticed for 2,7-CB-TDP (2.1693 eV) in the gas phase. This can be clarified by the conjugate length and strong electron donor giver character of the separate acceptor group in TDP. It is also realizing that since the solvent impact on the π-conjugated monomer has turned into the eventually liable for charged transport.

The estimations of the energy of the HOMO, LUMO and E_{gap} of all monomers are shown in Table-2 and in the following order: 2,7-CB-BCS > 2,7-CB-BCO > 2,7-CB-BCT > 2,7-CB-SCP > 2,7-CB-TCP > 2,7-CB-SDP > 2,7-CB-TDP > 2,7-CB-ODP > 2,7-CB-OCP. Besides, the littlest bandgap energy has been noticed for 2,7-CB-OCP (1.9946 eV). Contrasting and the gas and solvent phase, it is noted that the bandgap energies distinctive order. At long last, these outcomes show the impact of the solvent of the distinctive acceptor groups connected to the giver on the HOMO and LUMO energies on the electronic properties of the studied D-A monomers.

Photovoltaic properties: The active layer, the sufficient energy levels, and the best possible areas of HOMO and LUMO orbitals of organic molecules are needed and contrasted in the bulk heterojunction (BHJ) solar cells, and the LUMO energy level of the electron acceptor PBCM, which is commonly used in organic solar cells. The HOMO and LUMO orbitals are especially fascinating since they are engaged with the electron changes, in which the photoinduced electron moves from the energized state atom to the electron acceptor (PBCM). As shown in Fig. 5, it is noticed that the LUMO levels of all D-A monomers have high energies compare to PCBM LUMO energies. Along these lines, the electron moves from the considered atoms to the conduction band of PCBM are conceivable.

The active layer, the sufficient energy levels, and the best possible areas of HOMO and LUMO orbitals of organic molecules are needed and contrasted in the bulk heterojunction (BHJ) solar cells and the LUMO energy level of the electron acceptor PBCM, which is commonly used in organic solar cells. The HOMO and LUMO orbitals are especially fascinating since they are engaged with the electron changes, in which the photoinduced electron moves from the energized state atom to the electron acceptor (PBCM). As appeared in Fig. 5, noticed that the LUMO levels of all D-A monomers have high energies compare to PCBM LUMO energies. Along these lines, the electron moves from the considered atoms to the conduction band of PCBM are conceivable.

$$V_{oc} = |E_{HOMO}\,(Donor)| - |E_{LUMO}\,(Acceptor)| - 0.3$$

The V_{oc} estimations of considered D-A monomers mixed with the acceptors PCBM and C_{60}-OMe appear in Table-3. The determined V_{oc} values were in range from 2.16 to 2.94 eV concerning PCBM and from 2.34 to 2.73 eV concerning C_{60}-OMe in the gas phase and 1.53 to 1.86 eV for PCBM and 2.33 to 2.66 eV with respect to C_{60}-OMe in chlorobenzene solvent. The V_{OC} qualities are bigger than 0 eV, which guarantees productive electron move from the giver to the acceptor. Accordingly, all D-A monomers can be utilized as BHJ due to the electron infusion measure from the energized particle to the conduction band of the acceptor (PCBM/C_{60}-OMe).

Absorption properties: The UV absorption spectral properties of organic material are a significant factor for the application as a photovoltaic material, and a decent photovoltaic material must have wide and extraordinary obvious retention

TABLE-3
ENERGY VALUES OF E_{HOMO}, E_{LUMO} AND THE OPEN CIRCUIT VOLTAGE V_{oc} BY eV

D-A Polymer monomers	Gas				Chlorobenzene			
	HOMO (eV)	LUMO (eV)	V_{OC}		HOMO (eV)	LUMO (eV)	V_{OC}	
			PBCM	C60-OMe			PBCM	C60-OMe
2,7-CB-BCO	-5.7240	-2.7783	2.94	2.52	-5.7129	-2.8739	1.71	2.51
2,7-CB-BCT	-5.7240	-2.7784	2.94	2.52	-5.5298	-2.7767	1.53	2.33
2,7-CB-BCS	-5.5398	-2.6641	2.87	2.34	-5.6144	-2.7253	1.61	2.41
2,7-CB-OCP	-5.8636	-3.2703	2.59	2.66	-5.6620	-3.6674	1.66	2.46
2,7-CB-TCP	-5.7281	-3.2246	2.50	2.53	-5.7134	-3.2562	1.71	2.51
2,7-CB-SCP	-5.6647	-3.1237	2.54	2.46	-5.6808	-3.1378	1.68	2.48
2,7-CB-ODP	-5.9336	-3.6578	2.27	2.73	-5.8587	-3.6851	1.86	2.66
2,7-CB-TDP	-5.7763	-3.6070	2.16	2.58	-5.7684	-3.5898	1.77	2.57
2,7-CB-SDP	-5.7053	-3.4997	2.20	2.51	-5.7276	-3.4674	1.73	2.53
PCBM	-6.1000	-3.7000	–	–	–	–	–	–
C60-OMe	–	-2.9000	–	–	–	–	–	–

attributes. Beginning with enhanced optimized geometry, the electronic absorption spectra of the studied D-A monomers in the gas are calculated by utilizing TD-DFT/B3LYPmethod with a 6-31G(d) basis set. Tables 4 and 5 present the absorption spectra properties for all studied D-A monomers. The relating reproduced UV-vis spectra of all examinations D-A monomers, introduced as oscillator strength against intensity have appeared in Figs. 6 and 7 in gas and solvent phase, respectively. Excitation

TABLE-4
MAIN ELECTRON TRANSITIONS, WAVE LENGTHS (λ_{max}), OSCILLATOR STRENGTHS (f) AND CONTRIBUTION OF MOLECULAR ORBITAL CHARTER (%) for D-A MONOMERS BY USING TD-DFT/B3LYP WITH 6-31G(d) BASIS SET IN GAS PHASE

D-A monomer	State	λ_{max}	f	MO character (%)
2,7-CB-BCO	S1	500.71	0.0047	HOMO → LUMO (98.85)
	S2	468.36	0.2252	HOMO-1 → LUMO (98.56)
	S3	330.02	0.0238	HOMO-3 → LUMO (5.54)
				HOMO-2 → LUMO (90.45)
2,7-CB-BCT	S1	515.36	0.1221	HOMO → LUMO (99.09)
	S2	446.60	0.0055	HOMO-1 → LUMO (98.94)
	S3	363.28	0.0164	HOMO-2 → LUMO (97.51)
2,7-CB-BCS	S1	515.49	0.0115	HOMO-1 → LUMO (2.41)
				HOMO → LUMO (96.71)
	S2	499.05	0.1429	HOMO-1 → LUMO (96.61)
				HOMO → LUMO (2.33)
	S3	352.09	0.0058	HOMO-2 → LUMO (96.32)
2,7-CB-OCP	S1	525.05	0.0014	HOMO → LUMO (98.25)
	S2	500.95	0.1524	HOMO-1 LUMO (98.47)
	S3	394.57	0.0005	HOMO-4 → LUMO (97.66)
2,7-CB-TCP	S1	606.28	0.0029	HOMO → LUMO (99.24)
	S2	557.29	0.1385	HOMO-1 → LUMO (99.06)
	S3	418.38	0.0011	HOMO-4 → LUMO (91.91)
				HOMO-3→ LUMO (3.60)
				HOMO-2 → LUMO (3.39)
2,7-CB-SCP	S1	595.47	0.0030	HOMO → LUMO (99.28)
	S2	554.91	0.1377	HOMO-1 → LUMO (99.07)
	S3	423.35	0.0009	HOMO-4 → LUMO 78.80
				HOMO-3→ LUMO 17.07
				HOMO-2 → LUMO 3.10
2,7-CB-ODP	S1	686.63	0.0020	HOMO → LUMO 99.34
	S2	554.23	0.2759	HOMO-1 → LUMO 99.47
	S3	537.06	0.0000	HOMO-2 → LUMO 99.43
2,7-CB-TDP	S1	728.44	0.0015	HOMO → LUMO 99.26
	S2	597.83	0.2247	HOMO-1 → LUMO 99.36
	S3	582.68	0.0000	HOMO-2 → LUMO 99.49
2,7-CB-SDP	S1	713.34	0.0016	HOMO → LUMO 99.20
	S2	594.35	0.2177	HOMO-1 → LUMO 99.27
	S3	585.32	0.0000	HOMO-2 → LUMO 99.49

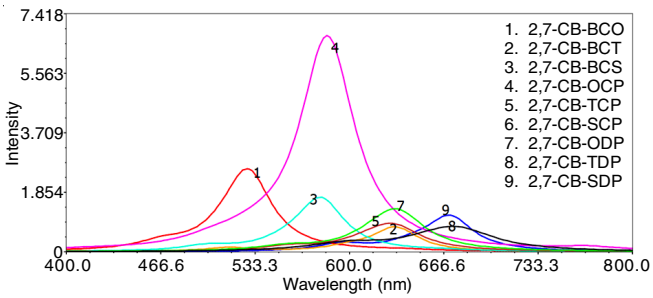

Fig. 6. Calculated UV-vis absorption spectra of D-A monomers by using TD-DFT/B3LYP with 6-31G (d) basis set in gas phase

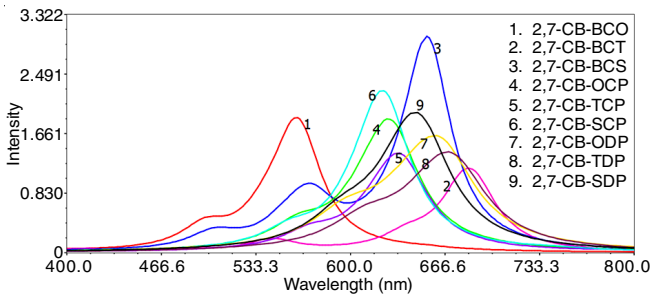

Fig. 7. Calculated UV-vis absorption spectra of D-A monomers by using TD-DFT/B3LYP with 6-31G(d) basis set in chlorobenzene solvent

to the S_1 state compares solely to the advancement of an electron from the HOMO to the LUMO orbital and is owing to the π-π* progress. The absorption intensities emerging from the $S_0 \rightarrow S_1$ electronic change increment continuously with the expanding of the electron giver strength substituents and with the diminishing of the bandgap energies of the D-A monomers. Table-5 and Fig. 6 show that there is a bathochromic move when passing from 2,7-CB-BCO (500.71 nm) to molecule 2,7-CB-TDP (728.44 nm) in the accompanying request: 2,7-CB-BCO →2,7-CB-BCS → 2,7-CB-BCT→2,7-CB-OCP→2,7-CB-SCP→2,7-CB-TCP→2,7-CB-ODP→2,7-CB-SDP→2,7-CB-TDP gas stage. In the solvent phase a bathochromic move when passing from molecule 2,7-CB-BCS (514.38 nm) to molecule 2,7-CB-TDP (725.31 nm) in the accompanying request: 2,7-CB-

TABLE-5
MAIN ELECTRON TRANSITIONS, WAVE LENGTHS (λ_{max}), OSCILLATOR STRENGTHS (f) AND CONTRIBUTION OF MOLECULAR ORBITAL CHARTER (%) for D-A MONOMERS BY USING TD-DFT/B3LYP WITH 6-31G(D) BASIS SET IN GAS PHASE

D-A monomer	State	λ_{max}	f	MO character (%)
2,7-CB-BCO	S1	524.28	0.0100	HOMO→ LUMO (99.26)
	S2	497.41	0.2903	HOMO-1 → LUMO (99.42)
	S3	341.69	0.0248	HOMO-3 → LUMO (2.31)
				HOMO-2 → LUMO (95.17)
2,7-CB-BCT	S1	545.06	0.1660	HOMO → LUMO (98.97)
	S2	457.88	0.0094	HOMO-1 → LUMO (98.92)
	S3	373.64	0.0235	HOMO-2 → LUMO (97.94)
2,7-CB-BCS	S1	514.38	0.0471	HOMO-1 → LUMO (2.40)
				HOMO → LUMO (96.72)
	S2	502.22	0.1799	HOMO-1 → LUMO (96.87)
				HOMO → LUMO (2.44)
	S3	355.11	0.0070	HOMO-2 → LUMO (97.32)
2,7-CB-OCP	S1	623.53	0.0053	HOMO → LUMO (99.37)
	S2	563.69	0.2804	HOMO-1 → LUMO (99.49)
	S3	389.25	0.0015	HOMO-4 → LUMO (93.83)
				HOMO-3 → LUMO (2.34)
				HOMO-2 → LUMO (2.61)
2,7-CB-TCP	S1	620.96	0.0066	HOMO → LUMO (99.31)
	S2	571.96	0.2052	HOMO-1 → LUMO (99.19)
	S3	403.07	0.0014	HOMO-4 → LUMO (95.71)
				HOMO-2 → LUMO (2.07)
2,7-CB-SCP	S1	595.41	0.0079	HOMO → LUMO (99.20)
	S2	557.36	0.2095	HOMO-1 → LUMO (99.22)
	S3	403.56	0.0012	HOMO-4 → LUMO (95.45)
				HOMO-3 → LUMO (2.74)
2,7-CB-ODP	S1	729.42	0.0035	HOMO → LUMO (99.45)
	S2	597.37	0.4226	HOMO-1 → LUMO (99.76)
	S3	509.18	0.0000	HOMO-2 → LUMO (99.39)
2,7-CB-TDP	S1	725.31	0.0028	HOMO → LUMO (99.43)
	S2	610.69	0.3596	HOMO-1 → LUMO (99.62)
	S3	530.48	0.0000	HOMO-2 → LUMO (99.41)
2,7-CB-SDP	S1	692.04	0.0030	HOMO → LUMO (99.41)
	S2	593.87	0.3544	HOMO-1 → LUMO (99.55)
	S3	525.75	0.0000	HOMO-2 → LUMO (99.39

BCS→2,7-CB-BCO→2,7-CB-BCT→2,7-CB-SCP→2,7-CB-TCP→2,7-CB-OCP→2,7-CB-SDP→2,7-CB- ODP→2,7-CB-TDP.

Conclusion

In present work, the D-A monomers design and the geometry optimization structures, optoelectronic properties by using DFT and TD-DFT methods with 6-31G(d) basis set calculations. The calculated bandgap values were in the range of 2.1693-2.9457 eV in the gas phase and 1.9946-2.8390 eV in the solvent phase. The D-A monomer, 2,7-CB-TDP has a low bandgap energy (2.1693 eV) in gas and 2,7-CB-OCP (1.9946 eV) in the solvent phase. The electronic absorption properties have been acquired by utilizing the TD-DFT/B3LYP method with a 6-31G (d) basis set. The obtained λ_{max} is in the range from 500.71 to 728.44 nm in the gas and 514.38 to 725.31nm in the solvent phase. The photovoltaic estimations of V_{oc} of the examined monomers range from in the gas phase was 2.16 to 2.94 eV/PCBM, from 2.34 to 2.66 eV/C_{60}-OMe and from 1.53 to 1.86 eV/PCBM and 2.33 to 2.66 eV/C_{60}-OMe in the dissolvable stage. These qualities are adequate for conceivable effective electron infusion from the energized monomers to the conduction band of PCBM/C_{60}-OMe. Finally, the results show how the electronic properties can be tuned with a few acceptor meetings by the substituent and suggest these mixes as a great contender for optoelectronic applications, such as BHJ in sun-powered cells, specifically the 2,7-CB-OCP monomer.

ACKNOWLEDGEMENTS

The authors declare that there is no conflict of interests regarding the publication of this article.

REFERENCES

1. S. Chaudhuri, M. Mohanan, A.V. Willems, J.A. Bertke and N. Gavvalapalli, *Chem. Sci*., **10**, 5976 (2019); https://doi.org/10.1039/C9SC01724K
2. A.K. Mishra, *J. Atom. Mol. Conden. Nano Phys*., **5**, 159 (2018); https://doi.org/10.26713/jamcnp.v5i2.842
3. K. Namsheer and C.S. Rout, *RSC Adv*., **11**, 5659 (2021); https://doi.org/10.1039/D0RA07800J
4. A. Upadhyay and S. Karpagam, *Rev. Chem. Eng*., **35**, 351 (2019); https://doi.org/10.1515/revce-2017-0024
5. L. Luo, W. Huang, C. Yang, J. Zhang and Q. Zhang, *Front. Phys.*, **16**, 33500 (2021); https://doi.org/10.1007/s11467-020-1045-6
6. H. Hong, R. Sfez, S. Yitzchaik and D. Davidov, *Synth. Met.*, **102**, 1217 (1999); https://doi.org/10.1016/S0379-6779(98)01278-8
7. B. Hu, Z. Yang and F.E. Karasz, *J. Appl. Phys.*, **76**, 2419 (1994); https://doi.org/10.1063/1.358458
8. Y. Ohmori, H. Kajii, T. Sawatani, H. Ueta and K. Yoshino, *Thin Solid Films*, **393**, 407 (2001); https://doi.org/10.1016/S0040-6090(01)01128-2
9. C. Liang, W. Li, Z. Hong, X. Liu, J. Peng, L. Liu, Z. Lu, M. Xie, Z. Liu, J. Yu and D. Zhao, *Synth. Met.*, **91**, 151 (1997); https://doi.org/10.1016/S0379-6779(97)04000-9
10. C.L. Lee, K.B. Lee and J.J. Kim, *Mater. Sci. Eng. B*, **85**, 228 (2001); https://doi.org/10.1016/S0921-5107(01)00592-X
11. S. Lamansky, R.C. Kwong, M. Nugent, P.I. Djurovich and M.E. Thompson, *Org. Electron.*, **2**, 53 (2001); https://doi.org/10.1016/S1566-1199(01)00007-6
12. J. Li and A.C. Grimsdale, *Chem. Soc. Rev.*, **39**, 2399 (2010); https://doi.org/10.1039/b915995a
13. S. Beaupré, P.L.T. Boudreault and M. Leclerc, *Adv. Mater.*, **22**, E6 (2010); https://doi.org/10.1002/adma.200903484
14. P.L.T. Boudreault, S. Beaupré and M. Leclerc, *Polym. Chem.*, **1**, 127 (2010); https://doi.org/10.1039/B9PY00236G
15. W.-Y. Wong and P.D. Harvey, *Macromol. Rapid Commun.*, **31**, 671 (2010); https://doi.org/10.1002/marc.200900690
16. S. Beaupré and M.J. Leclerc, *J. Mater. Chem.*, **1**, 11097 (2013); https://doi.org/10.1039/c3ta12420g
17. T. Michinobu, K. Okoshi, H. Osako, H. Kumazawa and K. Shigehara, *Polymer*, **49**, 192 (2008); https://doi.org/10.1016/j.polymer.2007.11.022
18. B. Cai, Y. Xing, Z. Yang, W.H. Zhang and J. Qiu, *Energy Environ. Sci.*, **6**, 1480 (2013); https://doi.org/10.1039/c3ee40343b
19. F. Dumur, *Org. Electron.*, **25**, 345 (2015); https://doi.org/10.1016/j.orgel.2015.07.007
20. J.F. Morin and M. Leclerc, *Macromolecules*, **34**, 4680 (2001); https://doi.org/10.1021/ma010152u
21. F. Dierschke, A.C. Grimsdale and K. Müllen, *Synthesis*, 2470 (2003); https://doi.org/10.1055/s-2003-42418
22. Z. Ma, L. Chen, J. Ding, L. Wang, X. Jing and F. Wang, *Adv. Mater.*, **23**, 3726 (2011); https://doi.org/10.1002/adma.201102140
23. S.G. Hahm, T.J. Lee, D.M. Kim, W. Kwon, Y.G. Ko, T. Michinobu and M. Ree, *J. Phys. Chem. C*, **115**, 21954 (2011); https://doi.org/10.1021/jp207211e
24. F. Lombeck, H. Komber, A. Sepe, R.H. Friend and M. Sommer, *Macromolecules*, **48**, 7851 (2015); https://doi.org/10.1021/acs.macromol.5b01845
25. B. Berns and B. Tieke, *Polym. Chem.*, **6**, 4887 (2015); https://doi.org/10.1039/C5PY00713E
26. A. El-Alamy, A. Amine and M. Bouachrine, *Orbital Electron. J. Chem.*, **7**, 327 (2015); https://doi.org/10.17807/orbital.v7i4.763
27. A.D. Becke, *J. Chem. Phys.*, **98**, 5648 (1993); https://doi.org/10.1063/1.464913
28. S. Miertus, E. Scrocco and J. Tomasi, *Chem. Phys.*, **55**, 117 (1981); https://doi.org/10.1016/0301-0104(81)85090-2
29. E. Cances, B. Mennucci and J. Tomasi, *J. Chem. Phys.*, **107**, 3032 (1997); https://doi.org/10.1063/1.474659
30. M. Zerner, K.B. Lipkowitz and D.B. Boyd, eds., VCH, New York, vol. 2, 313 (1991).
31. A. El Alamy, M. Bourass, A. Amine and M. Bouachrine, *Karbala Int. J. Modern Sci.*, **3**, 75 (2017); https://doi.org/10.1016/j.kijoms.2017.03.002
32. A. El alamy, A. El Ghaoury, A. Amine and M. Bouachrine, *J. Taibah Univ. Sci.*, **11**, 930 (2017); https://doi.org/10.1016/j.jtusci.2016.10.008
33. S.V. Meille, A. Farina, F. Bezziccheri and M.C. Gallazzi, *Adv. Mater.*, **6**, 848 (1994); https://doi.org/10.1002/adma.19940061109